



HHS Public Access

Author manuscript

J Morphol. Author manuscript; available in PMC 2020 April 25.

Published in final edited form as:

J Morphol. 1997 December ; 234(3): 263–276. doi:10.1002/(SICI)1097-4687(199712)234:3<263::AID-JMOR5>3.0.CO;2-A.

Development of the *Xenopus laevis* VIIIth cranial nerve: Increase in number and area of axons of the saccular and papillar branches

Vincent L. López-Anaya, Daniel López-Maldonado, Elba E. Serrano*

Department of Biology, New Mexico State University, Las Cruces, New Mexico, 88003

Abstract

Development of three branches of the VIIIth cranial nerve was examined in the anuran, *Xenopus laevis*. Sectioned tissue from the saccular, amphibian papillar, and basilar papillar branches of stage 52 larvae, one day post-metamorphosis juveniles, and two year adult animals was analyzed under the light microscope with a digital image analysis system. Numbers and cross-sectional areas of myelinated axons were measured in five to six nerve sections at each developmental age for each of the three branches. In all three branches, results show a significant increase in axon numbers between larval stage 52 and juvenile ages, and negligible increase in axon number between the juvenile and adult ages. There were differences in the average number of axons between the saccular (704.4 ± 39.5 ; $n = 5$), amphibian papillar (508.4 ± 35.0 ; $n = 5$), and basilar papillar (316.0 ± 7.0 ; $n = 5$) branches of adult animals. Myelinated axons increase at an estimated rate of 11.7, 15.1, and 6.2 axons per day for the saccular, amphibian papillar, and basilar papillar branches respectively. Axonal cross-sectional areas increased throughout the developmental ages of this study, with the greatest increase taking place between juvenile and adult ages. In adult animals, 98% of axons in all three branches have diameters between 2–10 μm . Ratios of axons to hair cells in adult animals were estimated at 0.3, 1.1, and 5.3 for the sacculus, amphibian papilla, and basilar papilla respectively. The higher axon to hair cell ratio correlates with the increasing acoustical frequency sensitivity of the end organ.

Keywords

Amphibian; Amphibian papilla; Anuran; Basilar papilla; Hair cell; Inner ear; Neuroanatomy; Sacculus

Anurans have long been the subject of intensive inquiry as a model for understanding the auditory and vestibular systems of vertebrates (Duellman and Trueb, '86). Physiological studies of the anuran VIIIth cranial nerve have shed light on the encoding and processing of

*To whom reprint requests should be addressed Send correspondence to: Dr. E. E. Serrano, Dept. of Biology, New Mexico State University, Las Cruces, NM, 88003. Tel No. (575) 646-5217; FAX (575) 646-5665; serrano@nmsu.edu.

Publisher's Disclaimer: "This is the peer reviewed version of the following article: López-Anaya, V. L., López-Maldonado, D. and Serrano, E. E. (1997), Development of the *Xenopus laevis* VIIIth cranial nerve: Increase in number and area of axons of the saccular and papillar branches (*J. Morphol.*, 234: 263–276), which has been published in final form at doi:10.1002/(SICI)1097-4687(199712)234:3<263::AID-JMOR5>3.0.CO;2-A. This article may be used for non-commercial purposes in accordance with Wiley Terms and Conditions for Use of Self-Archived Versions."

acoustical signals (Feng et al., '75; Wilczynski and Capranica, '84; Baird and Lewis, '86; Zakon and Wilczynski, '88). Anatomical studies of the innervation of the anuran ear have characterized the sensory fields of VIIIth nerve fibers (Lewis et al., '82a; Honrubia et al., '89; Simmons et al., '92; Baird and Schuff, '94), providing evidence for reciprocal synapses between inner ear hair cells and afferent fibers (Dunn, '78) and for efferent innervation of the sensory epithelia (Robbins et al., '67; Will and Fritzsche, '88; Hellman and Fritzsche, '96). Anuran auditory and vestibular hair cells are a valuable model system for understanding the signal transduction mechanisms that underlie mechanoreception (Hudspeth and Gillespie, '94; Shepherd and Corey, '94), electrical responses (Lewis and Hudspeth, '83; Ashmore and Pitchford, '85; Housley et al., '89; Baird, '92), and transmitter release (Roberts et al., '91; Issa and Hudspeth, '96) in hair cells of the inner ear. Furthermore, there is evidence that hair cells of the anuran sensory epithelia are produced throughout adult life (Lewis and Li, '73; Corwin, '85; Díaz et al., '95). Anurans are capable of regenerating hair cells (Baird et al., '93; Baird et al., '96), and VIIIth cranial nerve fibers can regenerate after experimental damage (Zakon and Capranica, '81; Zakon, '83; Zakon, '88). Thus, in addition to providing important information about acoustic communication and signal transduction, anurans are a viable model for studies of proliferation and regeneration in nerve fibers and hair cells.

The majority of these studies have focused on the properties of mature ears from adult anurans, especially those of ranid frogs such as *Rana catesbeiana* and *Rana pipiens*. Much less is known about the physiology (Shofner and Feng, '81), anatomy (Shofner and Feng, '84; Corwin, '85; Fritzsche et al., '88; Will and Fritzsche, '88; Hellman and Fritzsche, '96), and gene expression (Gallagher et al., '96) that occur during development of the anuran inner ear. In particular, the role of the VIIIth cranial nerve in development and maintenance of the sensory epithelia requires further investigation (Fritzsche et al., '88).

Recent studies in rodents have shown that innervation of the sensory epithelia by the VIIIth cranial nerve requires neurotrophins such as brain-derived neurotrophic factor (BDNF) and neurotrophin-3 (NT-3), and their cognate receptors trkB and trkC (Pirvola et al., '94; Ernfors et al., '95; Bianchi et al., '96). While there is evidence that the initial morphological maturation of hair cells does not require innervation (Fritzsche et al., '97), the role of the nerve in the physiological maturation of hair cells and the maintenance of normal sensory epithelial function is less well understood. Our laboratory is investigating the events that underlie the morphological and physiological differentiation of the sensory epithelia, such as the development of hair cell stereociliary bundles (Diaz et al., '95), synapse formation, and the acquisition of ion channels and signal transduction pathways by hair cells (Trujillo-Provencio et al., '97). One goal of our research is to determine whether the VIIIth cranial nerve influences the functional development of inner ear hair cells.

We have chosen *Xenopus laevis* as the organism for our investigations of amphibian ear development. The development of *X. laevis* from oocyte to adult has been thoroughly documented (Nieuwkoop and Faber, '67) and this organism is a well-established, classical system for cellular and molecular studies (Kay and Peng, '91; Tinsley and Kobel, '96). However, while some data are available about acoustical processing by *X. laevis* (Vigny, '79; Elepfandt, '96) and gross anatomy of the *X. laevis* ear (Paterson, '49; Nieuwkoop and Faber, '67), detailed information about the sensory hair cells of *X. laevis* and their innervation is

scarce (see however Baird, '74; Lewis, '78; Will and Fritzs, '88; Fritzs et al., '88; Díaz et al., '95; Hellman and Fritzs, '96), especially when compared with what is known about other anurans.

Like the ears of other anurans (Geisler et al., '64; Feng et al., '75), the inner ear of *Xenopus laevis* has eight sensory structures (Paterson, '49) that are innervated by branches of the VIIIth cranial nerve (Fig. 1). In this study we characterized the development of the three branches of the VIIIth cranial nerve that innervate the sacculus (SAC), the amphibian papilla (AP), and the basilar papilla (BP). Physiological and anatomical studies in anurans have shown that these three sensory end organs are specialized for reception of acoustical signals of different frequencies (Lewis et al., '82a; Duellman and Trueb, '86). *X. laevis* responds to acoustical frequencies between 200–3900 Hz, a range comparable to that of similarly sized terrestrial anurans (Elepfandt, '96). High frequencies (>1000 Hz) are perceived by the BP, intermediate frequencies (100–1400 Hz) by the AP, and low frequencies (<300 Hz) by the SAC (Lewis et al., '82a; Zakon and Wilczynski, '88).

Understanding of the role of the VIIIth cranial nerve during formation of the sensory epithelia requires knowledge about the pattern of axon growth during inner ear development. To this end, we obtained quantitative data about the myelinated axons of the SAC, AP, and BP branches of the VIIIth cranial nerve during *Xenopus laevis* development. We used a digital image analysis system to analyze sectioned nerve branches under the light microscope, and characterized axon growth by measuring the numbers and cross-sectional areas of axons. Data were collected from axons in the nerve branches of 5–6 animals at three different ages: larval stage 52, juvenile animals at one day post-metamorphosis, and two year adult animals.

Our results provide quantitative, comparative data about the development of three branches of the VIIIth cranial nerve, and show important similarities and differences between myelinated fibers of the three branches. In particular, results suggest that like in other anurans, the three sensory end organs differ from one another in the richness of their innervation as measured by estimates of axon to hair cell ratios (Will and Fritzs, '88; Fritzs et al., '88; Simmons et al., '92). Furthermore, a higher axon to hair cell ratio is correlated with a higher frequency sensitivity of the end organ.

MATERIALS AND METHODS

Collection of nerve specimens and sensory end organs

The animals ($n = 47$) used in this study represent approximately two years of *Xenopus laevis* life. Animals were bred in our colony or purchased from a commercial supplier (Nasco, Fort Atkinson, WI). At stage 52 (staged according to Nieuwkoop and Faber, '67), the SAC and papillar branches of the VIIIth cranial nerve can be distinguished as individual branches and readily microdissected with their sensory end organs from the inner ear (Fig. 1). At this stage, myelinated axons can be clearly identified under the light microscope. Therefore, this larval stage was chosen as the youngest age for our developmental studies. Sacculi and auditory papillae, together with their nerve branches, were removed from stage 52 larvae (0.2 – 0.3 gm), juvenile animals (0.8 – 1 gm) that were one day post metamorphosis, and

adults (40 – 60 gm; 7.5–10 cm). The animal ages were the same as those we used in a previous study of SAC hair cell addition during *X. laevis* development (Díaz et al., '95), allowing comparison of SAC axon data with SAC hair cell data from the same age. According to the supplier, adult animals were approximately two years old. Larvae and juveniles were not sexed and were randomly selected from tanks where animals grew into adults of both genders in roughly equal numbers. Both male and female adults were included in the study. Experimental procedures were approved by the Institutional Animal Care and Use Committee of New Mexico State University.

Tissue preparation

Animals were anesthetized with a 4°C solution of 0.1% (larvae) or 0.2% (juveniles and adults) 3-aminobenzoic acid ethyl ester methanesulfonate salt (Sigma, A5040), and then decapitated. The heads were placed in frog Ringer's solution (115mM NaCl, 2.0 mM KCl, 2.0 mM CaCl₂, 1.5 mM NaHCO₃, 10mM HEPES, pH 7.4) with the ventral side facing up. The otic capsules were approached through the exposed roof of the mouth with the aid of a dissecting microscope (Nikon SMZ-2T). If necessary, the lower jaw was removed. Using fine forceps and a surgical scalpel, the base of the skull was removed, exposing the otic capsule and the ventral aspect of the brain where the VIIIth cranial nerve exits the medulla oblongata. The ventral floor of the otic capsules was removed and the VIIIth cranial nerve was severed at the entrance to the otic capsule. The entire inner ear was removed by grasping the anterior ramus of the VIIIth cranial nerve in a pair of fine forceps.

For SAC specimens, the nerve branch and its sensory end organ were microdissected from the inner ears, and the tissue placed in a dialdehydic fixative solution (1.5% paraformaldehyde, 2.5% glutaraldehyde, 0.1 M sodium cacodylate, pH 7.4) for 15–24 h at 4°C. For the smaller, more delicate auditory papillae, the entire otic capsules (larvae and juveniles) or the inner ears (adults) were surgically removed and fixed (see above) 15–24 h at 4°C prior to final microdissection.

After fixation, the specimens were submerged in a decalcifying buffer solution (0.1 M cacodylate, 0.1 M EDTA, pH 7.4) three times (15 min each wash), to remove the residual otolithic crystals. The organs then were given three washes of 15 min each (0.1 M cacodylate, pH 7.4), and post-fixed (2.0% osmium tetroxide, 0.1 M cacodylate buffer, pH 7.4) for 30–60 min, then washed 4 times for 15 min (0.1 M cacodylate, pH 7.4). After post-fixing, the tissue was dehydrated with increasingly higher concentrations of ethanol, 50% (15 min), 70% (15 min), 95% (5 times, 15 min each), 100% (4 times, 15 min each). The papillar branches of the VIIIth cranial nerve together with their sensory end organs were microdissected from the labyrinth of the opened otic capsules, or from the inner ears, in 70% ethanol solution following the 70% ethanol dehydration step, then the dehydration schedule was resumed. After dehydration, ethanol was cleared and the tissue was embedded in ARALDITE 502/EMbed 812 (EMS 13940) according to the manufacturer's instructions. Specimens were oriented in the block in a consistent manner, then placed in a 70°C oven for 24 h to cure.

Transverse sections (1 µm) of each branch were prepared for the light microscope for data analysis using glass knives (LKB Ultratome III 8801A Microtome). Every fifth (papillar

branches) or tenth (SAC branch) section was mounted on a gelatin-subbed slide. Sections were stained with Methylene Blue 1% (EMS 18600) for 30–45 sec and then rinsed in double distilled water. To obtain maximum contrast for better digital image analysis, sections were deliberately overstained, covered with a single large cover slip, then viewed and analyzed with a Nikon TMD inverted microscope at 400× or 1000×. Sections were photographed at 200×, 400× or 1000× with a Zeiss Axophot microscope under brightfield illumination.

Digital image analysis of nerve branches

Five to six sections were analyzed for each age group from each of the three nerve branches. In order to be consistent when comparing data from different branches, the data were collected by analyzing the sectioned tissue at a specific region of the nerve branch (Fig. 2). As *Xenopus laevis* matures from stage 52 to adult, there is an increase in the size of the inner ear, the length of the VIIIth cranial nerve and its branches, and the distance between individual end organs. However, the gross morphology of the inner ear remains similar throughout development, and location of the inner ear end organs on the VIIIth cranial nerve was therefore comparable between the three age groups (Fig. 1).

Sections of the SAC branch were analyzed at the point of entry to the SAC (Fig. 2A). In the AP branch, the amphibian papillar contact membrane and the papillo-saccular foramen served as landmarks, providing a consistent plane present in the three ages through which to section the nerve branch for analysis (Fig. 2B). Data collected from the BP branch were analyzed at the point of entry to the cartilaginous ring of the organ (Fig. 2C).

Images of sections were viewed through a CCD camera (SONY AVC-D7) mounted to the cineport of a Nikon Diaphot TMD inverted microscope. Images were displayed on a color monitor (SONY Trinitron), and permanently stored on video using a VCR (SONY DA Pro 4 Head) connected in series between the camera and the monitor. Images from the CCD camera or stored video images were captured and digitized for data analysis with a videographics adapter board (Truevision Targa+) in a ZEOS 486 computer using an image acquisition and analysis program (JAVA Videoanalysis system, Jandel Scientific, Corte Madera, CA). The captured images were saved as TIF files. Digitized images were further magnified and enhanced to improve resolution prior to analysis (Fig. 3).

Once a suitable image was acquired, the JAVA program was used to determine the total number of axons in the section (Table 1), and the circumference and cross-sectional area of each axon (Fig. 3). Data represent measurements collected from myelinated axons, as the light microscope cannot reliably resolve unmyelinated axons (Baird and Schuff '94). Data were saved as ASCII files and imported into the QUATTRO PRO (Borland International) or MICROSOFT EXCEL (Microsoft Corporation) program for further analysis and graphics preparation. Axon numbers and cross-sectional areas are given as mean \pm standard error (S.E.). An advantage of using a digital image analysis system is that reported values are measurements of actual areas, regardless of the shape of the axons, and are not calculated from estimates of axon diameter (Ewart et al., '89). To prepare Table 2, axon areas from each analyzed nerve branch section were grouped into bins, and the averages for each bin were calculated for each branch at each developmental age. The equivalent axon diameters (μm) corresponding to the bin axon areas were calculated geometrically (Ewart et al., '89).

Differences between the means of data sets were statistically evaluated using the two-tailed Student's *t*-test.

RESULTS

Morphological Development of the Saccular and Papillar Branches

Saccular Branch—Our microdissection of the SAC indicates that this organ is innervated by the anterior and posterior branches of the VIIIth cranial nerve (see Fritzsche et al., '88), an innervation pattern resembling that of the terrestrial frog, *Rana catesbeiana* (Feng et al., '75), but unlike that of *Rana pipiens* (Simmons et al., '92). The innervation originates from the point where these two rami bifurcate from the trunk of the VIIIth cranial nerve (Fig. 1).

In stage 52 larvae, the SAC axons are lightly stained and are grouped as 2–5 bundles (Fig. 4A). At the juvenile age of development, the axons show more distinct separation into 6–8 bundles, comprising more axons (Fig. 4B), and the nerve branch assumes an oblong shape that is also characteristic of adult specimens. In the mature adult (Fig. 4C), the axons of the SAC branch are segregated into 7–14 bundles that continue to branch as they approach the sensory organ. A similar morphology has been observed in *Rana catesbeiana* (Dunn, '78).

Amphibian Papillar Branch—The AP branch of the VIIIth cranial nerve maintains a close association with its end organ as it loops down, around this pod-like structure, terminating at the end of a 180° turn (Fig. 2B). The AP branch originates from the posterior ramus of the VIIIth cranial nerve (Fig. 1). In some sections the endolymphatic duct is observed, as previously reported in *Rana catesbeiana* (Wilczynski and Capranica, '84). This duct carries endolymph from the expansive endolymphatic sac outside the otic capsule to the lumen of the labyrinth.

Sectioned tissue from the AP branches of stage 52 larvae shows very few, lightly stained axons that form an long ellipsoid bundle that is closely associated with the epithelial cells that form the posterior wall of the papilla (Fig. 5A). In most juvenile sections, the nerve branch retains its ellipsoid shape (Fig. 5B), although in one specimen the branch was divided in two smaller ellipsoid bundles of unequal size, a pattern that is not observed in other specimens of any age. Adult AP branches assume an oblong shape, and are visibly less elongated than sections observed in earlier ages (Fig. 5C). In contrast with stage 52 nerve branches (Fig. 5A), the juvenile and adult branches form more cohesive bundles with a much more uniform distribution of similarly sized axons (Fig. 5B,C).

Basilar Papillar Branch—The BP branch projects from the posterior ramus of the VIIIth cranial nerve (Fig. 1) and enters the cartilaginous ring of the end organ (Fig. 2C). The BP branch of stage 52 larvae typically comprises a few lightly stained axons (Fig. 6A) that are grouped in 2–4 bundles. In the juvenile, this nerve branch appears as an elongated and bent ellipse (Fig. 6B) that in one specimen is fully crescent shaped. In two juvenile specimens, the BP branch gives the appearance of two discrete ellipsoid bundles that are joined together at the apex of their respective long axes (Fig. 6B). Axons within these bundles are remarkably uniform in size, with small areas of smaller, lightly stained axons distributed within the body of the bundle. In the adult, the BP branch is characteristically crescent

shaped, and contains a preponderance of similarly sized axons (Fig. 6C). Also, the BP branch in adult specimens demonstrates more consistent morphology than in the specimens from the two earlier ages.

Comparative Morphology of the Saccular and Papillar Branches

In *Xenopus laevis*, the SAC, BP, and AP receive innervation from the posterior ramus of the VIIIth cranial nerve; the SAC also receives innervation from the anterior ramus (Fig. 1). The peripheral distribution of nerve branches to the SAC and the BP in *X. laevis* is believed to represent a morphologic series of changes from what is presumed to be the primitive innervation pattern of urodelian and gymnophian amphibians. In particular, the anuran BP branching pattern and fiber distribution reflects an evolutionary trend which is considered a derived character state not seen in reptiles and mammals (Will and Fritzsich, '88).

In juvenile and adult specimens, the morphology of transverse sections of the SAC branch of the VIIIth cranial nerve differs from that of the AP and BP branches. The axons of AP (Fig. 5B,C) and BP (Fig. 6B,C) branches tend to form a single, continuous axon bundle from the posterior ramus of the VIIIth cranial nerve until approaching their respective sensory macula, where they begin to branch apart before terminating within their end organ. The BP branch is the smallest of the three nerve branches. The SAC branch (Fig. 4B,C) is easily distinguished from its papillar counterparts (Figs. 5B,C, 6B,C) by its larger size, and by the aggregation of its axons into many distinct bundles. The BP branch shows comparatively greater variability than the AP branch. In some adult sections, the AP branch appears as a larger and more cohesive bundle than the BP branch. The SAC branch shows the least variability in morphology of all three branches at each age, while the BP branch shows the greatest variability between specimens at all ages. In stage 52 larvae, the axons of the SAC and papillar branches are sparsely myelinated and hence lightly stained (Figs. 4A, 5A, 6A). In contrast, juvenile branches comprise well myelinated and darkly stained axons (Figs. 4B, 5B, 6B), suggesting that significant myelination has occurred by the juvenile age.

Increase in Axon Numbers

The SAC (Fig. 4B) and papillar (Figs. 5B, 6B) branches in juvenile specimens have greater cross-sectional areas than corresponding branches from stage 52 larvae (Figs. 4A, 5A, 6A), reflecting the developmental increase in myelinated axon number (Table 1, Fig. 7). Between stage 52 and the juvenile age, the average axon number increases by 3.3× in the SAC branch, by 14.2× in the AP branch, and by 4.2× in the BP branch. The average number of axons present in each branch at stage 52 is significantly different ($p^* < 0.002$) from that of the juvenile (Fig. 7). In the adult, the SAC is innervated by 704.4 ± 39.5 ($n = 5$) axons, the AP by 508.4 ± 35.0 ($n = 5$) axons, and the BP by 316.0 ± 7.0 ($n = 5$) axons (Fig. 7). The average number of axons present in each branch at the juvenile age is not significantly different ($p < 0.10$) from that of the same branch at the adult age.

Increase in Axon Area

Axons in sectioned tissue are mostly elliptical in shape (Figs. 3, 5–7). The average axon areas of all three branches increase throughout the developmental ages included in this

study. Furthermore, there are observable differences in the pattern of increase between the three branches (Fig. 8, Table 2).

For the SAC branch, there is no significant increase in the average axon area between stage 52 larvae ($10.64 \pm 0.95 \mu\text{m}^2$; $n = 5$) and juvenile ($11.69 \pm 0.15 \mu\text{m}^2$; $n = 5$), but there is a significant increase ($p^* < 0.01$) of 1.5 \times between the juvenile and the adult ($17.72 \pm 1.18 \mu\text{m}^2$; $n = 5$). For the AP branch, there is a significant increase ($p^{***} < 0.0001$) of 1.8 \times in the average axon area between stage 52 larvae ($2.94 \pm 0.17 \mu\text{m}^2$; $n = 6$) and juvenile ($5.17 \pm 0.15 \mu\text{m}^2$; $n = 5$), and a significant ($p^* < 0.01$) and even larger increase of 4.7 \times between the juvenile and adult specimens ($24.14 \pm 3.40 \mu\text{m}^2$; $n = 5$). For the BP branch, there is a significant increase ($p^{**} < 0.001$) of 3.1 \times in the axon area of sections between stage 52 larvae ($2.47 \pm 0.33 \mu\text{m}^2$; $n = 6$) and juvenile ($7.63 \pm 0.70 \mu\text{m}^2$; $n = 5$), and also ($p^* < 0.01$) between the juvenile and adult ($14.82 \pm 1.43 \mu\text{m}^2$; $n = 5$).

In comparing the three branches, it is apparent that the AP branch undergoes the greatest developmental increase in the axon area, and this occurs chiefly between juvenile and adult ages, although an increase is evident between stage 52 and juvenile (Table 2, Fig. 8). The axon area of the BP branch increases progressively with age, while axons of the SAC branch increase in area mainly between the juvenile and adult (Table 2, Fig. 8).

In Table 2 the SAC and papillar axons are grouped into bins on the basis of cross-sectional area at each developmental age. The data for the BP quantitatively show that in this branch, the average axon area is more narrowly distributed than in the other two branches. For example, in adult specimens, 74.7 % of the axons have average diameters between 3–5 μm ; this increase was apparent from visual inspection of the sections before analysis (Fig. 6C). Furthermore, the AP and SAC branches are notable for containing a small population (~ 1 –2 %) of very large axons with diameters greater than 10 μm . In adult, axons with diameters greater than 5 μm comprised 48.2%, 27.7%, and 18.2 % of the axons of the AP, SAC, and BP, respectively (Table 2).

DISCUSSION

Developmental increase in axon numbers and axon areas

Over a two year period of *Xenopus laevis* life, we observed developmental increases in the number (Table 1, Fig. 7) and size (Table 2, Fig. 8) of the myelinated axons of the AP, BP, and SAC branches of the VIIIth cranial nerve. In particular, from stage 52 larvae to the juvenile age, there is a pronounced increase in the number of axons of the three branches of the VIIIth cranial nerve, most notably for the AP branch (Table 1, Fig. 7). Cellular processes that may account for this increase include myelination of existing axons (not discernible with light microscopy in larval animals), the addition of new cells to the VIIIth cranial nerve ganglia (Will and Fritzsche, '88), or increased arborization of terminals during development (Baird and Schuff, '94). There is no significant increase in the number of axons between juvenile and adult *X. laevis* (Table 1, Fig. 7).

Larval and juvenile animals were bred in our laboratory, consequently we could use the specimen's age to estimate the rate of increase in myelinated axons during this

developmental interval. Approximately 36 days elapsed between larval stage 52 and the juvenile age. Thus we estimate increases of 11.7, 15.1, and 6.2 myelinated axons per day for the SAC, AP, and BP respectively, underscoring a difference in axon growth between the branches.

The increase in axon size follows a different time course from the increase in axon number. For all three branches, but most notably the AP branch, axon size increases during the two year period (Table 2, Fig. 8). Developmental increase in axon size leads to an increase in the conduction velocity of adult axons relative to those of stage 52 larvae. A faster conduction velocity can offset the increase in distance between cells and their nerve terminals (Dunn, '78). The mechanism underlying the developmental changes in axon area may involve interactions between VIIIth nerve axons and the sensory epithelia, since recent studies suggest that retrograde signals from target tissues may be important in regulating axon size and myelination (Voyvodic, '89; Yin and Oppenheim, '92; Xiong et al., '94).

Axon diameters

At all ages, the three branches studied could be distinguished from one another by the characteristic diameter distribution of their axon populations. For example, in adult *Xenopus laevis*, 92% of SAC axons, 84% of AP axons and 98% of BP axons have diameters in the range 2–7 μm (Table 2). The adult AP branch has more axons with diameters greater than 7 μm than either the SAC or BP branch. However the SAC branch contains the most axons with diameters greater than 10 μm . Differences in the axon diameter distributions of adult SAC, AP, and BP branches have previously been shown for *Rana catesbeiana* (Geisler et al., '64; Dunn, '78). In this species, large diameter (>10 μm) fibers are also numerous in the SAC branch. At present, the functional significance of these larger diameter fibers is unclear (Dunn, '78).

Relationships between axons and hair cells

This study was prompted by our interest in the role of the VIIIth cranial nerve in differentiation of the inner ear sensory epithelia. The attainment of a proper convergence between VIIIth nerve axons and hair cells is an important process that takes place during synaptogenesis in the developing sensory epithelia (Lewis et al., '82b; Fritzsche et al., '88; Simmons et al., '92). Since knowledge of the ratio of VIIIth nerve axons to hair cells during development is a fundamental step towards understanding synapse formation, we performed calculations using our data and the reported values from the literature to estimate these ratios for the three sensory end organs.

Data about the number of hair cells during development of the *Xenopus laevis* AP and BP are not available. However, results from an earlier study of SAC development from our laboratory showed that SAC hair cell addition is greatest during larval stages, estimated at 26 hair cells per day, and declining to about 0.5 hair cells per day after the juvenile age (Díaz et al., '95). We estimate that the increase in myelinated axons of the SAC branch is greatest during the early developmental period (prior to the juvenile age, at approximately 11.7 axons per day) and negligible afterward (Table 1, Fig. 7). Taken together, the data suggest that the juvenile age is preceded by significant, concomitant developmental increases in the numbers

of SAC hair cells and SAC myelinated axons. The numbers of hair cells in the sacculi of stage 52, juvenile, and adult *X. laevis* have been measured at 1100, 2084, and 2460 respectively (Díaz et al., '95). We estimate the ratio of axons to hair cells at 0.16 in stage 52 larvae, and slightly greater at 0.29 in the juvenile and adult *X. laevis*. The higher ratio reflects the fact that the number of axons increases by 3.9× while the number of hair cells increases by only 2.2× during this period.

In adult *Xenopus laevis*, the number of hair cells is estimated at 400–500 in the AP and 50–70 in the BP (Baird, '74; Lewis, '78; Elepfandt, '96). We used our numbers for axons in SAC and papillar branches of adult animals to estimate the ratio of axons to hair cells for each sensory end organ. Ratios of 0.3, 1.1, and 5.3, were calculated for the adult SAC, AP, and BP respectively. Similar ratios have been estimated for the AP and BP of ranid species (Frishkopf and Flock, '74; Will and Fritzsich, '88; Simmons et al., '92). The high ratio of 4–5 axons to hair cells underscores the divergent innervation (multiple nerve fibers contact a single hair cell) of the BP and has prompted analogy with the inner hair cells of the organ of Corti (Frishkopf and Flock, '74).

In anurans, the SAC fibers typically respond to low frequency acoustical and vibrational stimuli of less than 300 Hz, while the AP fibers respond to intermediate acoustical frequencies of 100–1400 Hz, and the BP fibers respond best to acoustical frequencies between 1000–4000 Hz (Lewis et al., '82a; Zakon and Wilczynski, '88). The AP exhibits tonotopicity and it has been suggested that the traveling wave model of the cochlea may also be present (Lewis et al., '82b). Thus in anurans like *Xenopus laevis*, the increase in axon to hair cell ratio appears to parallel the increase in frequency sensitivity of the three sensory end organs.

There is evidence for differences in the innervation of the end organs between anurans. Will and Fritzsich ('88) have noted differences in the peripheral branching pattern of the VIIIth cranial nerve between anurans such as *Ascaphus truei*, *Bombina orientalis*, *Bufo bufo*, and *Xenopus laevis*. Until recently, it was believed that all end organs in anurans except the BP received efferent innervation (Robbins et al., '67; Frishkopf and Flock, '74; Will and Fritzsich, '88). However, acetylcholinesterase-positive fibers have been identified in the *X. laevis* BP, suggesting the presence of efferent fibers in the end organ of this species (Hellman and Fritzsich, '96). Comparisons of the convergence between axons and hair cells show additional innervation differences between anurans. In *Rana catesbeiana*, a BP fiber typically innervates one hair cell (Lewis et al., '82a), but a BP fiber of *Rana pipiens* often can contact up to 5 hair cells (Simmons et al., '92). The innervation of the AP appears to be similar in *R. pipiens* and *R. catesbeiana*; each nerve fiber has been shown to contact several (1–15) hair cells (Lewis et al., '82a; Simmons et al., '92). Information about the formation of synaptic connections between VIIIth nerve axons and hair cells of the *X. laevis* SAC, AP, and BP is scarce, and will be the theme of future developmental studies.

Xenopus laevis, like other anurans, continues to produce hair cells throughout its life (Lewis and Li, '73; Corwin, '85; Díaz et al., '95), which can be over thirty years (Tinsley and Kobel, '96). In contrast, the number of myelinated axons does not increase significantly after the juvenile age (Table 1, Fig. 7). However, there is evidence that at least in papillar end

organs, physiological changes are occurring during anuran inner ear development as the animal continues to grow to adult following metamorphosis. Data from electrical recordings indicate that frequency responses of BP and AP fibers are different between recently metamorphosed and adult *Rana catesbeiana* (Shofner and Feng, '81). Further investigation is required to determine how the innervation patterns, sensory fields, and physiology of the VIIIth nerve axons are modulated during development and aging of the sensory epithelia of the inner ear (Fritzsche et al., '88).

Summary

Our results show that during development of the *Xenopus laevis* VIIIth cranial nerve, increase in myelinated axons in the SAC, AP, and BP branches occurs primarily prior to one day post-metamorphosis. An increase in the axon areas of the three branches is observed throughout the life of the animal, with the greatest increase during the period following metamorphosis. The three branches can be distinguished from one another on the basis of morphology, rates of axon increase, estimated ratios of axons to hair cells, and the distribution of fiber diameters. In future experiments we will extend our investigations of the *X. laevis* inner ear to ultrastructural and physiological studies of the development of the innervation of the sensory epithelia.

ACKNOWLEDGMENTS

We are grateful to Hank Adams and Mark Cunningham, of the NMSU Electron Microscope Laboratory for their patience, time, and expertise, and to Dr. Peter Narins for encouragement and helpful discussions during the course of this research and the preparation of the manuscript. V. L. L. and D. L. are NIH MBRS trainees. This research was supported by NIH (MBRS S06-GM08136-18; NIDCD RO3 DC01460-01) and Whitehall Foundation grants to EES.

LITERATURE CITED

- Ashmore JF, and Pitchford S (1985) Evidence for electrical resonant tuning in hair cells of the frog amphibian papilla. *J. Physiol* 364: 39.
- Baird IL (1974) Some aspects of the comparative anatomy and evolution of the inner ear in submammalian vertebrates. *Brain Behav. Evoln* 10: 11-36.
- Baird RA (1992) Morphological and electrophysiological properties of hair cells in the bullfrog utricle. *Ann. NY Acad. Sci* 656: 12-26. [PubMed: 1599137]
- Baird RA, and Lewis ER (1986) Correspondences between afferent innervation patterns and response dynamics in the bullfrog utricle and lagena. *Brain Res.* 369: 48-64. [PubMed: 2870777]
- Baird RA, and Schuff NR (1994) Peripheral innervation patterns of vestibular nerve afferents in the bullfrog utricle. *J. Comp. Neurol* 342: 279-298. [PubMed: 8201035]
- Baird RA, Steyger PS, and Schuff NR (1996) Mitotic and nonmitotic hair cell regeneration in the bullfrog vestibular otolith organs. *Ann. N. Y. Acad. Sci* 781: 59-70. [PubMed: 8694449]
- Baird RA, Torres MA, and Schuff NR (1993) Hair cell regeneration in the bullfrog vestibular otolith organs following aminoglycoside toxicity. *Hear. Res* 65: 164-174. [PubMed: 8458749]
- Bianchi LM, Conover JC, Fritzsche B, DeChiara T, Lindsay RM, Yancopoulos GD (1996) Degeneration of vestibular neurons in late embryogenesis of both heterozygous and homozygous BDNF null mutant mice. *Development* 122:1965-1973. [PubMed: 8674435]
- Corwin JT (1985) Perpetual production of hair cells and maturational changes in hair cell ultrastructure accompany postembryonic growth in an amphibian ear. *Proc. Natl. Acad. Sci. USA* 82: 3911-3915. [PubMed: 3923484]

- Díaz ME, Varela-Ramírez A, and Serrano EE (1995) Quantity, bundle types, and distribution of hair cells in the sacculus of *Xenopus laevis* during development. *Hear. Res* 91: 33–42. [PubMed: 8647723]
- Duellman WE, and Trueb L (1986) *Biology of Amphibians*. Baltimore: The Johns Hopkins University Press.
- Dunn RF (1978) Nerve fibers of the eighth nerve and their distribution to the sensory nerves of the inner ear in the bullfrog. *Neurology* 182: 621–636.
- Elepfandt A (1996) Underwater acoustics and hearing in the clawed frog, *Xenopus*. In Tinsley RC and Kobel HR (eds): *The Biology of Xenopus*. Oxford: Clarendon Press, pp. 177–193.
- Ernfors P, Van de Water T, Loring J, and Jaenisch R (1995) Complementary roles of BDNF and NT-3 in vestibular and auditory development. *Neuron* 14:1153–1164. [PubMed: 7605630]
- Ewart DP, Kuzon WMJ, Fish JS, and McKee NH (1989) Nerve fiber morphometry: a comparison of techniques. *J. Neurosci. Met* 29: 143–150.
- Feng AS, Narins PM, and Capranica RR (1975) Three populations of primary auditory fibers in the bullfrog (*Rana catesbeiana*): their peripheral origins and frequency sensitivities. *J. Comp. Physiol* 100: 221–229.
- Frishkopf LS, and Flock Å (1974) Ultrastructure of the Basilar Papilla, an Auditory Organ in the Bullfrog. *Acta Otolaryng.* 77: 176–184. [PubMed: 4594555]
- Fritsch B, Silos-Santiago I, Bianchi LM, and Farinas I (1997) The role of neurotrophic factors in the development of inner ear innervation. *Trends. Neurosci* 20:159–164. [PubMed: 9106356]
- Fritsch B, Wahnschaffe U, and Bartsch U (1988) Metamorphic changes in the octavolateralis system of amphibians. In Fritsch B, Ryan MJ, Wilczynski W, Hetherington TE, and Walkowiak W (eds): *The Evolution of the Amphibian Auditory System*. New York: Wiley and Sons, pp. 359–376.
- Gallagher BC, Johnathan JH, and Grainger RM (1996) Inductive processes leading to inner ear formation during *Xenopus* development. *Dev. Biol* 175:95–107. [PubMed: 8608872]
- Geisler CD, van Bergeijk W, and Frishkopf LS (1964) The inner ear of the bullfrog. *J. Morphol* 114: 43–58. [PubMed: 14114962]
- Hellman B and Fritsch B (1996) Neuroanatomical and histochemical evidence for the presence of common lateral line and inner ear efferents to the basilar papilla in a frog, *Xenopus laevis*. *Brain Behav. Evol* 47:185–194. [PubMed: 9156781]
- Honrubia V, Hoffman LF, Sitko S, Schwartz IR (1989) Anatomic and physiological correlates in bullfrog vestibular nerve. *J. Neurophys* 61:688–701
- Housley GD, Norris CH, and Guth PS (1989) Electrophysiological properties and morphology of hair cells isolated from the semicircular canal of the frog. *Hear. Res* 38: 259–276. [PubMed: 2468636]
- Hudspeth AJ, and Gillespie PG (1994) Pulling springs to tune transduction: adaptation by hair cells. *Neuron* 12: 1–9. [PubMed: 8292354]
- Issa NP, and Hudspeth AJ (1996) The entry and clearance of Ca²⁺ at individual presynaptic active zones of hair cells from the bullfrog's sacculus. *Proc. Natl. Acad. Sci. USA* 93: 9527–9532. [PubMed: 8790364]
- Kay BK, and Peng HB (1991) *Xenopus laevis: Practical Uses in Cell and Molecular Biology*. Santa Barbara: Academic Press, Inc.
- Lewis ER (1978) Comparative studies of the anuran auditory papillae. *Scanning Electron Micros.* 2: 633–642.
- Lewis ER, Baird RA, Leverenz EL, and Koyama H (1982a) Inner ear: dye injection reveals peripheral origins of specific sensitivities. *Science* 215: 1641–1643. [PubMed: 6978525]
- Lewis ER, Leverenz EL, and Koyama H (1982b) The tonotopic organization of the bullfrog amphibian papilla, an auditory organ lacking a basilar membrane. *J. Comp. Physiol* 145: 437–445.
- Lewis ER, and Li CW (1973) Evidence concerning the morphogenesis of saccular receptors in the bullfrog (*Rana catesbeiana*). *J. Morphol* 139: 351–362. [PubMed: 4539709]
- Lewis RS, and Hudspeth AJ (1983) Voltage- and ion-dependent conductances in solitary vertebrate hair cells. *Nature* 304: 538–541. [PubMed: 6603579]
- Nieuwkoop PD, and Faber J (1967) *Normal Table of Xenopus laevis (Daudin)*. Amsterdam: North-Holland Publishing Co.

- Paterson NF (1949) The development of the inner ear of *Xenopus laevis*. Proc. Zool. Soc. Lond 119: 269–291.
- Pirvola U, Arumae U, Moshnyakov M, Palgi J, Saarma M, and Ylikoski J (1994) Coordinated expression and function of neurotrophins and their receptors in the rat inner ear during target innervation. Hear. Res 75:131–144. [PubMed: 8071140]
- Roberts WM, Jacobs RA, and Hudspeth AJ (1991) The hair cell as presynaptic terminal. Ann. N Y Acad. Sci 635: 221–233. [PubMed: 1660236]
- Robbins RG, Bauknight RS, and Honrubia V (1967) Anatomical distribution of efferent fibers in the VIIIth cranial nerve of the bullfrog (*Rana catesbeiana*). Acta Otolaryngol. 64:436–448. [PubMed: 5300212]
- Shepherd GM, and Corey DP (1994) The extent of adaptation in bullfrog saccular hair cells. J. Neurosci 14: 6217–6229. [PubMed: 7931574]
- Shofner WP, and Feng AS (1981) Post-metamorphic development of the frequency selectivities and sensitivities of the peripheral auditory system of the bullfrog, *Rana catesbeiana*. J. Exp. Biol 93: 181–196.
- Shofner WP, and Feng AS (1984) Quantitative light and scanning electron microscope study of the developing auditory organs in the bullfrog: implications on their functional characteristics. J. Comp. Neurol 224: 141–154. [PubMed: 6609173]
- Simmons DD, Bertolotto C, and Narins PM (1992) Innervation of the amphibian and basilar papillae in the leopard frog: reconstructions of single labeled fibers. J. Comp. Neurol 322: 191–200. [PubMed: 1522248]
- Tinsley RC and Kobel HR (1996) The Biology of *Xenopus*. Oxford: Clarendon Press.
- Trujillo-Provencio C, Varela-Ramirez A, Williams CE, Gladden JN, and Serrano EE (1997) RT-PCR analysis of gene expression in the *Xenopus laevis* inner ear: Actin and delayed rectifier potassium channels. ARO Abstr. 20:855.
- Vigny C (1979) The mating calls of 12 species and sub-species of the genus *Xenopus* (amphibia: Anura). J. Zool. Lond 188: 103–122.
- Voyvodic JT (1989) Target size regulates calibre and myelination of sympathetic axons. Nature 342: 430–433. [PubMed: 2586612]
- Wilczynski W, and Capranica RR (1984) The auditory system of anuran amphibians. Prog. Neurobiol 22: 1–38. [PubMed: 6374763]
- Will U, and Fritzsich B (1988) The eighth nerve of amphibians: peripheral and central distribution In Fritzsich B, Ryan MJ, Wilczynski W, Hetherington TE, and Walkowiak W (eds): The Evolution of the Amphibian Auditory System. New York: Wiley and Sons, pp. 159–184.
- Xiong M, Pallas SL, Lim S, and Finlay BL (1994) Regulation of retinal ganglion cell axon arbor size by target availability: mechanisms of compression and expansion of the retinotectal projection. J. Comp. Neurol 344: 581–597. [PubMed: 7929893]
- Yin Q, and Oppenheim R (1992) Modifications of motoneuron development following transplantation of thoracic spinal cord to the lumbar region in the chick embryo: evidence for target-derived signals that regulate differentiation. J. Neurobiol 23: 376–395. [PubMed: 1634886]
- Zakon H, and Capranica RR (1981) An anatomical and physiological study of regeneration of the eighth nerve in the leopard frog. Brain Res. 209: 325–338. [PubMed: 6971688]
- Zakon HH (1983) Reorganization of connectivity in amphibian central auditory system following VIIIth nerve regeneration time course. J. Neurophysiol 49: 1410–1427. [PubMed: 6603498]
- Zakon HH (1988) Regeneration in the amphibian auditory system In Fritzsich B, Ryan MJ, Wilczynski W, Hetherington TE, and Walkowiak W (eds): The Evolution of the Amphibian Auditory System. New York: Wiley and Sons, pp. 393–411.
- Zakon HH, and Wilczynski W (1988) The physiology of the anuran eighth nerve In Fritzsich B, Ryan MJ, Wilczynski W, Hetherington TE, and Walkowiak W (eds): The Evolution of the Amphibian Auditory System. New York: Wiley and Sons, pp. 159–184.

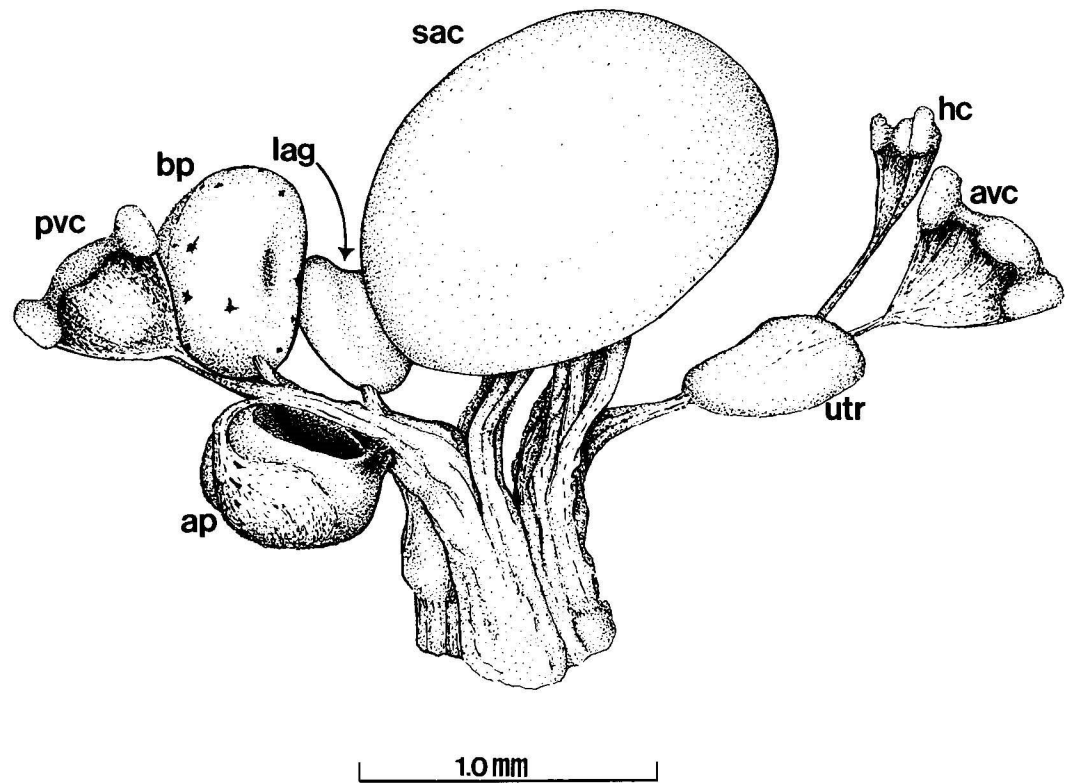


Fig. 1. Diagram of the end organs and nerve branches of the adult *Xenopus laevis* inner ear (left ear, dorsomedial aspect). Relative position and morphology of end organs and nerve branches depicted are consistent between ages, although dimensions vary in an age-dependent manner. Vestibular canals have been omitted to show positions of relevant structures. ap, amphibian papilla; avc, crista of the anterior vertical canal; bp, basilar papilla; hc, crista of the horizontal canal; lag, lagena; pvc, crista of the posterior vertical canal; sac, sacculus; utr, utricle.

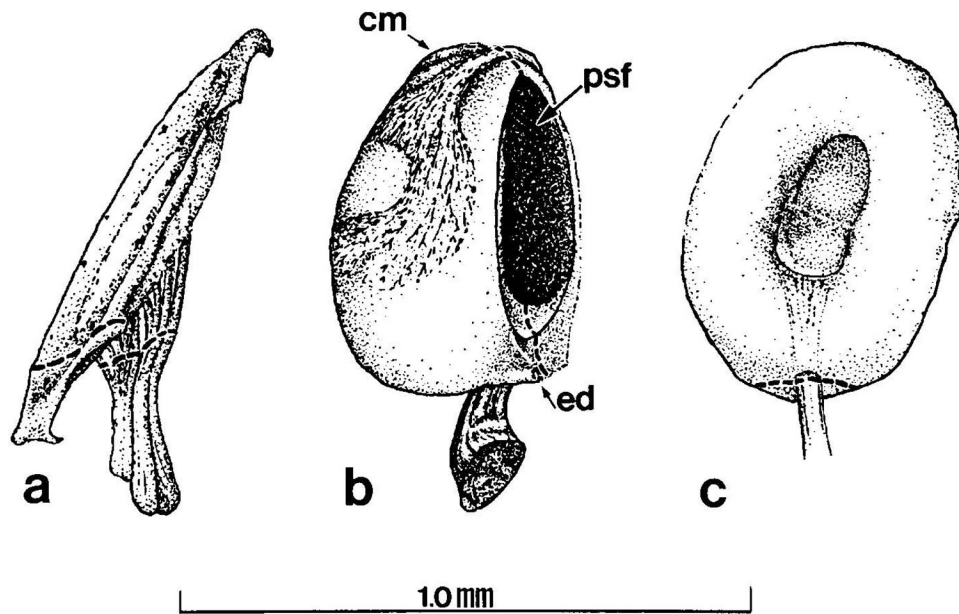


Fig. 2.

Three end organs of the adult *Xenopus laevis* inner ear examined in this study. Dashed lines through nerve branches indicate plane through which histological sections were made to collect data from all ages. Stage 52 larval and juvenile end organs are smaller than adult end organs but have the same morphology. (a) Sacculus: the saccular otolithic mass is removed to show comparative size of the end organ. (b) Amphibian papilla. (c) Basilar papilla. cm, contact membrane; ed, endolymphatic duct; psf, aperture of the papillo-saccular foramen.

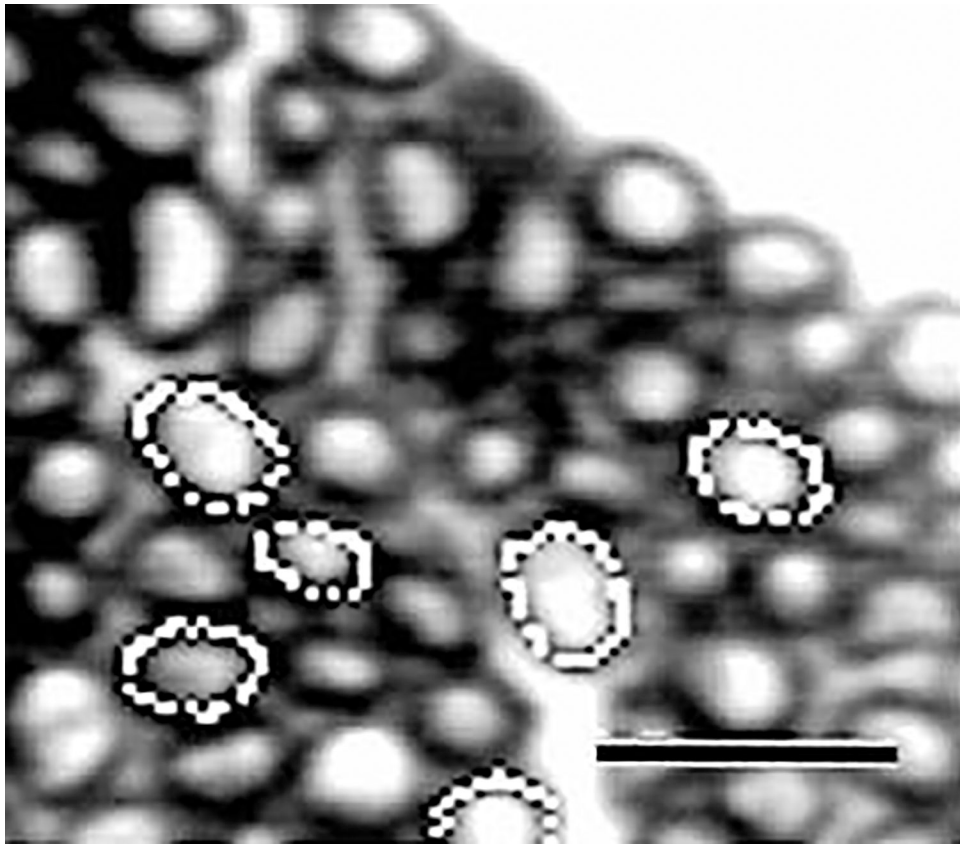


Fig. 3. *Xenopus laevis*. Digitized image showing enlarged area of a transverse section from an adult basilar papillar branch. Images were captured, then magnified, enhanced, and analyzed using a digitizing image analysis system. Light circles indicate traced axon circumference. Bar = 10 μm .

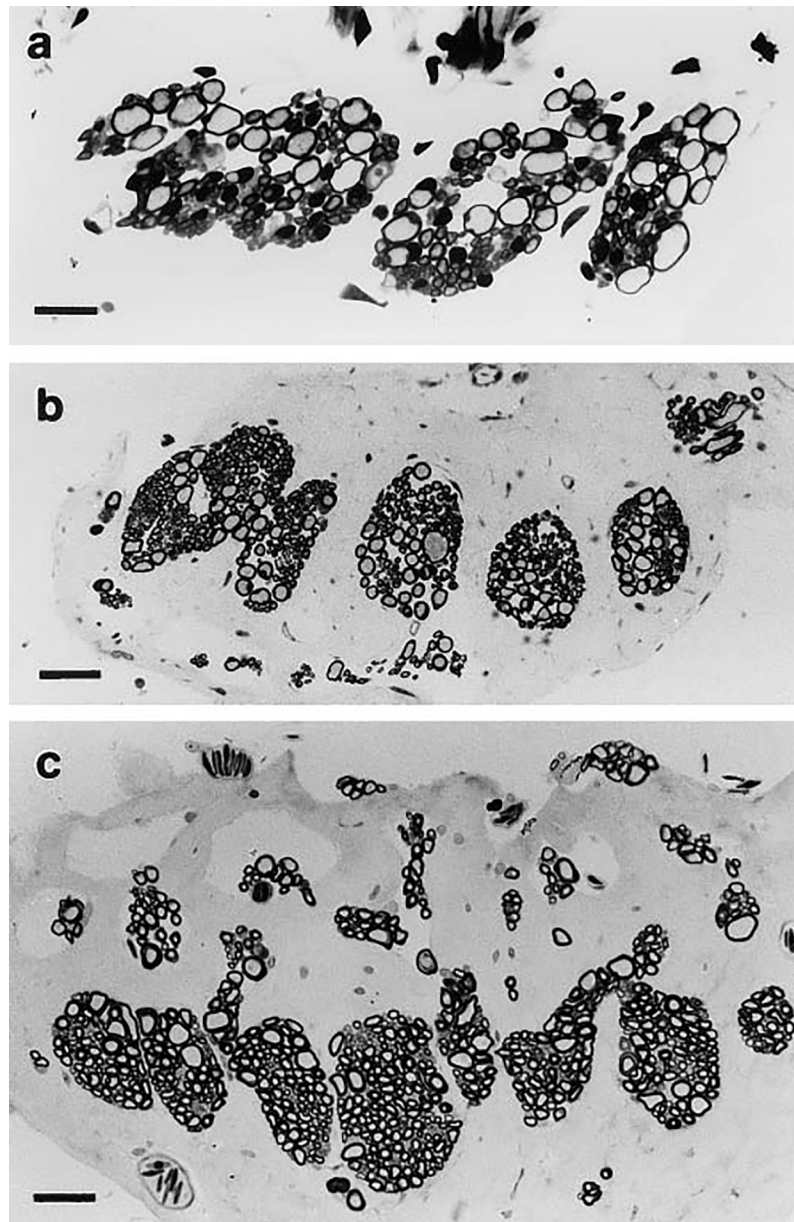


Fig. 4. Light micrographs of transverse sections of the saccular branch of the *Xenopus laevis* VIIIth cranial nerve. (a) Larval stage 52, (b) juvenile, 1 day postmetamorphosis, (c) adult. Bars = (a) 20 μm , (b,c) 40 μm .

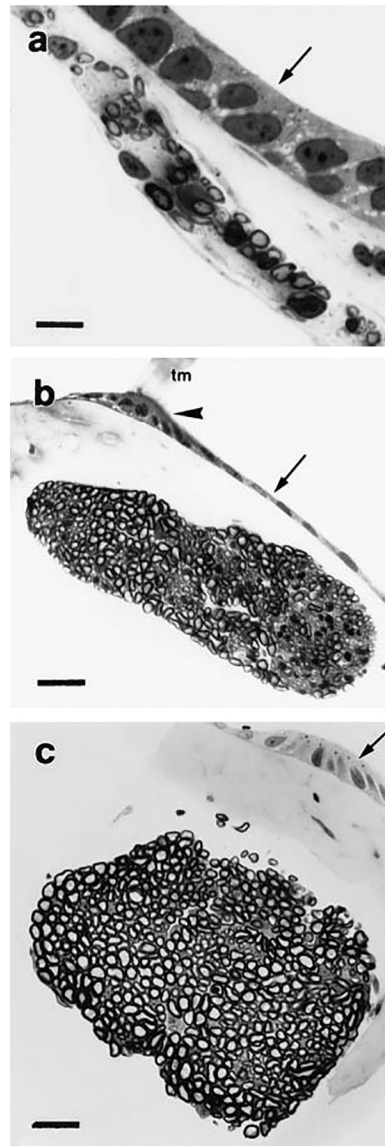


Fig. 5. (right) Light micrographs of transverse sections of the amphibian papillar branch of the *Xenopus laevis* VIIIth cranial nerve. Arrows indicate lumen of the papillar epithelium. Large arrowhead indicates the attachment point of the tectorial membrane. (a) Larval stage 52, (b) juvenile, 1 day postmetamorphosis, (c) adult. Bars = (a) 10 μm , (b,c) 25 μm . tm, tectorial membrane.

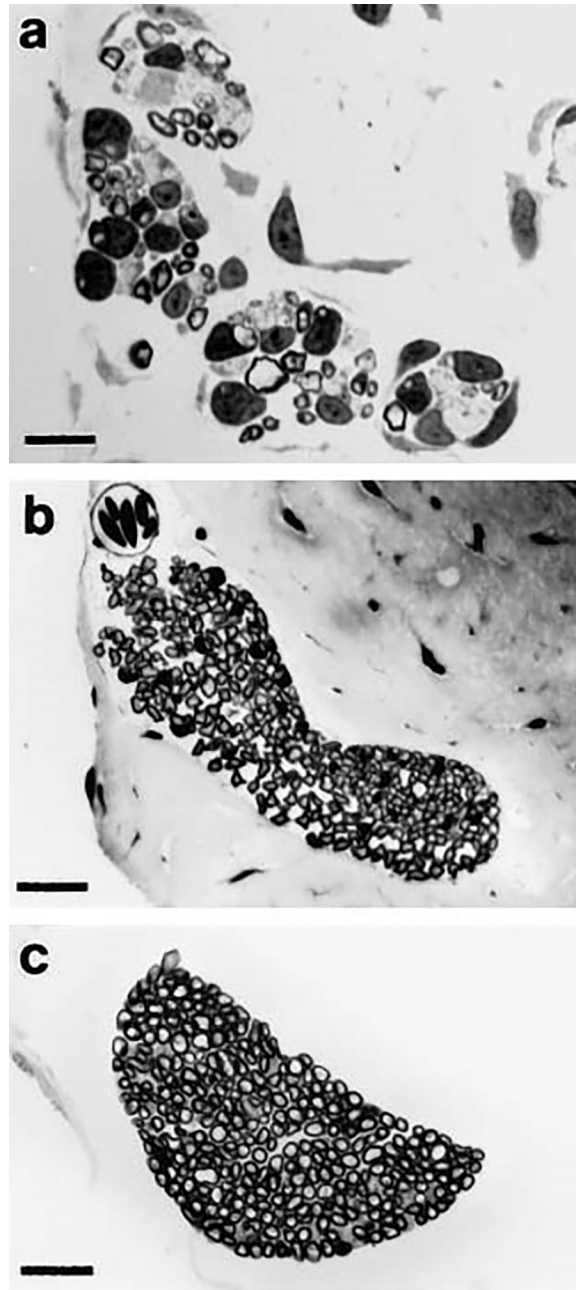


Fig. 6. Light micrographs of transverse sections of the basilar papillar branch of the *Xenopus laevis* VIIIth cranial nerve. (a) Larval stage 52, (b) juvenile, 1 day postmetamorphosis, (c) adult. An enlarged area of this section is shown in Figure 3. Bars = (a) 10 μm , (b,c) 25 μm .

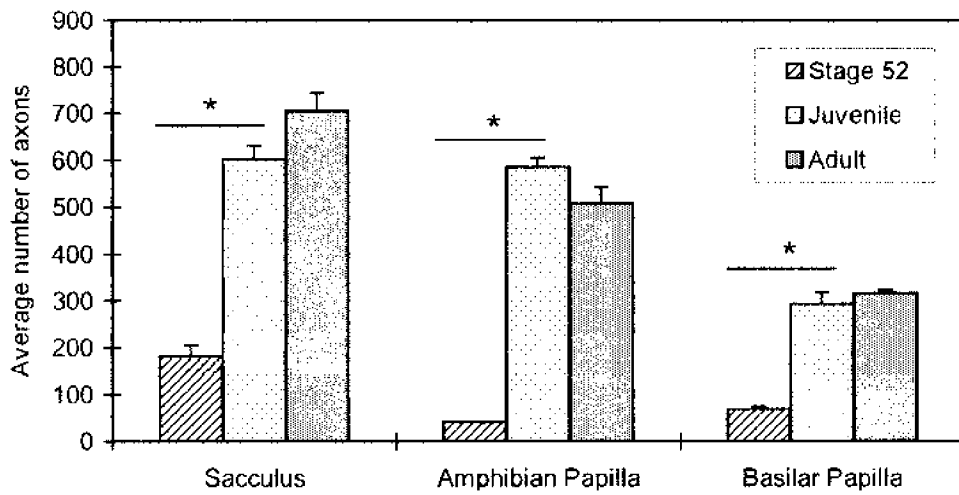


Fig. 7. Increase in the average number of myelinated axons (mean \pm S.E.) of the saccular, amphibian papillar and basilar papillar branches of the VIIIth cranial nerve during development of the *Xenopus laevis* inner ear. There is a significant difference in the number of axons between stage 52 and juvenile in the three end organs. *, $P < 0.002$.

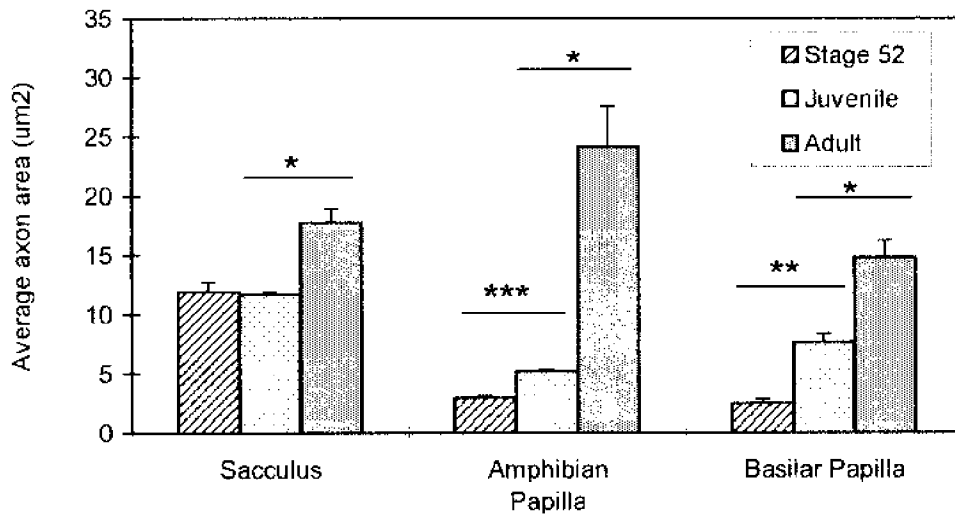


Fig. 8. Increase in the average area of axons (mean \pm S.E.) of the saccular, amphibian papillar and basilar papillar branches of the VIIIth cranial nerve during development of the *Xenopus laevis* inner ear. There is a significant difference in the area of axons between stage 52 and juvenile in the AP and BP, and between juvenile and adult in the three end organs. *, $P < 0.01$; **, $P < 0.001$; ***, $P < 0.0001$.

Table 1

Increase in the number of axons during development of the saccular and papillar branches of the *Xenopus laevis* VIIIth cranial nerve.

	Number of Axons		
	SACCULUS	AMPHIBIAN PAPILLA	BASILAR PAPILLA
Stage 52	138	39	87
(0.2–0.3 gm)	152	41	59
	129	41	58
	264	41	75
	225	42	69
		43	68
Juvenile	477	612	350
(0.8–1 gm)	624	514	239
	619	545	252
	615	621	251
	681	637	371
Adult	567	584	339
(40–60 gm)	692	467	295
	678	399	315
	836	481	327
	749	611	304

Average number of axons, their areas and diameters during development of the saccular and papillar branches of the *Xenopus laevis* VIIIth cranial nerve.

Table 2

	AXON AREA (μm^2):	0.79	Average Number of Axons*						
			>0.79 – 3.14	>3.14 – 7.07	>7.07 – 19.63	>19.63 – 38.48	>38.48 – 78.54	>78.54	
AXON DIAMETER (μm):	1	>1 – 2	>2 – 3	>3 – 5	>5 – 7	>7 – 10	>10		
Sacculus									
Stage 52	2.4 ± 0.7	48.6 ± 16.8	59.2 ± 8.3	38.6 ± 10.3	25.4 ± 5.8	7.2 ± 1.6	0.2 ± 0.2		
(n = 5)	(1.3%)	(26.8%)	(32.6%)	(21.3%)	(14.0%)	(4.0%)	(0.1%)		
Juvenile	0	40.6 ± 4.1	250.8 ± 19.4	230.6 ± 15.1	41.8 ± 3.9	37.6 ± 2.2	1.8 ± 0.7		
(n = 5)	-	(6.7%)	(41.6%)	(38.2%)	(6.9%)	(6.2%)	(0.3%)		
Adult	0	8.6 ± 1.5	134.4 ± 17.3	367.2 ± 20.2	145.8 ± 18.7	35.0 ± 5.1	14.0 ± 2.5		
(n = 5)	-	(1.2%)	(19.1%)	(52.1%)	(20.7%)	(5.0%)	(2.0%)		
Amphibian Papilla									
Stage 52	3.3 ± 1.9	22.0 ± 2.1	14.2 ± 1.9	1.7 ± 0.5	0	0	0		
(n = 6)	(8.1%)	(53.4%)	(34.4%)	(4.0%)	-	-	-		
Juvenile	15.0 ± 1.7	215.0 ± 11.1	201.6 ± 15.0	153.0 ± 10.4	1.2 ± 0.5	0	0		
(n = 5)	(2.6%)	(36.7%)	(34.4%)	(26.1%)	(0.2%)	-	-		
Adult	0	2.8 ± 1.9	40.0 ± 22.2	220.8 ± 50.8	164.2 ± 33.8	75.8 ± 25.0	5.2 ± 1.9		
(n = 5)	-	(0.6%)	(7.9%)	(43.4%)	(32.3%)	(14.9%)	(1.0%)		
Basilar Papilla									
Stage 52	9.0 ± 1.6	43.2 ± 4.6	14.2 ± 2.5	3.0 ± 1.6	0	0	0		
(n = 6)	(13.0%)	(62.3%)	(20.4%)	(4.3%)	-	-	-		
Juvenile	1.8 ± 1.0	41.4 ± 19.0	109.6 ± 15.8	137.0 ± 20.3	2.8 ± 1.5	0	0		
(n = 5)	(0.6%)	(14.1%)	(37.5%)	(46.8%)	(1.0%)	-	-		
Adult	0	2.4 ± 0.5	20.0 ± 4.3	236.2 ± 19.2	54.0 ± 20.6	3.4 ± 2.2	0		
(n = 5)	-	(0.8%)	(6.3%)	(74.7%)	(17.1%)	(1.1%)	-		

* Axons are grouped into seven bins by area (μm^2). The axonal areas from analyzed nerve branch sections were grouped into bins and then data for each bin was averaged for each age for each of the three branches. The axon diameters (μm) corresponding to the bin axon areas were calculated from the equation, $\text{area} = \pi r^2$. The relative number of axons for each branch at each age in a given bin are represented by percentages under the data for numbers of axons.